

PAPER • OPEN ACCESS

## Remarks on constitutive and structural modelling of small radii in sheet metal and crashworthiness simulation

To cite this article: A Haufe *et al* 2018 *IOP Conf. Ser.: Mater. Sci. Eng.* **418** 012124

View the [article online](#) for updates and enhancements.

You may also like

- [Investigation on crashworthiness and mechanism of a bionic antler-like gradient thin-walled structure](#)  
Zhiquan Wei, Xu Zhang and Yang Zheng
- [Optimized foam filling configuration in bi-tubular crush boxes: a comprehensive experimental and numerical analysis](#)  
Hamidreza Salaripour, Mohammadbagher B Azimi and Masoud Asgari
- [Crashworthiness of automobile made of HDPE/kenaf and HDPE/MWCNT polymer composites](#)  
Nayan Pundhir, Himanshu Pathak and Sunny Zafar



**ECS**  
The  
Electrochemical  
Society  
Advancing solid state &  
electrochemical science & technology

**DISCOVER**  
how sustainability  
intersects with  
electrochemistry & solid  
state science research

# Remarks on constitutive and structural modelling of small radii in sheet metal and crashworthiness simulation

A Haufe<sup>1</sup>, T Erhart<sup>1</sup>, F Andrade<sup>1</sup>, T Willmann<sup>2</sup> and M Bischoff<sup>2</sup>

<sup>1</sup>DYNAmore GmbH, Industriestrasse 2, D-70565 Stuttgart, Germany

<sup>2</sup>Institut für Baustatik und Baudynamik, Universität Stuttgart, Pfaffenwaldring 7, 70569 Stuttgart, Germany

{andre.haufe;tobias.erhart}@dynamore.de

{tobias.willmann;manfred.bischoff}@ibb.uni-stuttgart.de

**Abstract.** In recent years, one has seen a tremendous progress in methods for the simulation of production processes, especially in the automotive industry. Besides sheet metal forming, casting of alloys, moulding of polymers and various additive techniques are the key methods in manufacturing. In this list, sheet metal forming is unarguably the most mature virtual discipline to predict part producibility and the local properties. However, when it comes to transferring results from sheet metal forming simulation to further disciplines, like stiffness, NVH or crashworthiness simulation, a number of incompatibilities between the models need to be resolved. This is particularly pronounced when locally varying part properties are relevant. For situations in which the discrepancies in the constitutive models are not too dominating, this has been done successfully in the past by simply transferring thickness, plastic strain and possibly stresses, using shell elements in both disciplines. But since local effects, like extreme thinning, sharp bending or the onset of instability may dominate the fracture process in crashworthiness, especially when modern high strength alloys are regarded, these effects need to be investigated in more detail. In particular, their accurate evaluation may require modelling with 3D solid elements. On the one hand, the incompatibilities of the models become clearly obvious from the spatial discretization, while on the other the demand w.r.t. accuracy in crashworthiness is ever increasing. The present contribution focuses on the ability to capture demanding deformation states with classical and advanced shell formulations, which is seen as a first step in order to close the corresponding gap in the simulation process chain in a more general sense.

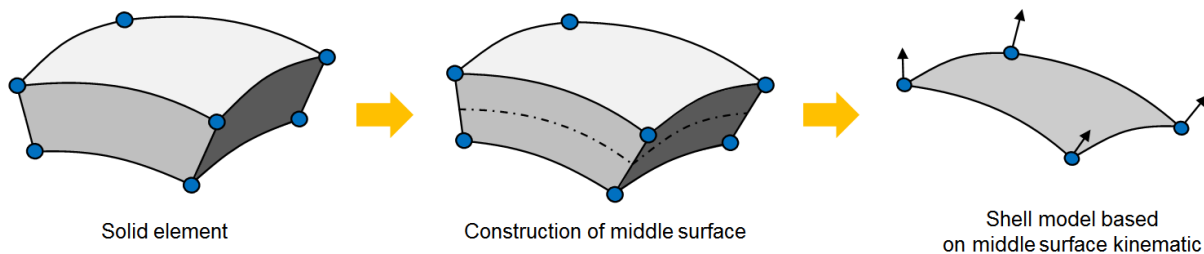
## 1. Introduction

In recent years, the quality in sheet metal forming simulation has achieved a remarkable level for many different applications, when appropriate constitutive laws and a corresponding spatial discretization were applied. However, due to new requirements, in particular emerging from design trends, the limits of the current shell model technology is almost reached. Worth mentioning in this context are so-called zero-radius edges or even sharp beads as proposed for state-of-the-art side panel designs in the automotive industry. This statement is to be seen in the context of customary applied spatial discretization with classical shell elements. In the following the basics of common shell models are discussed and the advantages and disadvantages of corresponding numerical implementations for the desired application are shown. Further hints and suggestions for dealing with alternative or enhanced spatial discretization technologies, such as so-called "thick" shell formulations or even volume elements, are given.



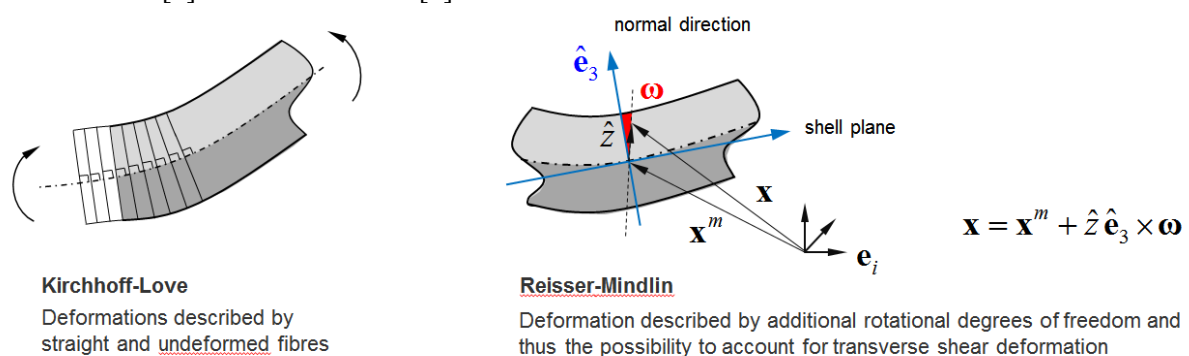
## 2. The state of the art in shell models

Classically, structures whose extension in two of their spatial directions is many times greater than in the third (thickness) direction are referred to as shells. As a measure of the typical aspect ratio that allows modelling on the basis of classical shells models, their *slenderness*, i.e. the length (or radius) to thickness ratio, is the crucial feature. This geometrically defined ratio allows justification of assumptions with regard to the mechanical description that are the basis of these shell models. From an engineering point of view, this is, on the one hand, the subordinate significance of stress components in the thickness direction and, on the other hand, the assumption of straight (undeformed) fibres in transverse direction during the deformation process. The literature, that deals with the derivation of such shell models and their basic assumptions, is manifold and will not be discussed in detail here. As an indication it should be sufficient to mention that most of the currently available implementations in commercial finite element software codes are usually based on the concept of degeneration (see figure 1) according to Ahmad et al. [1] or are motivated with the work of Koiter [2]. Their basic kinematic assumptions are also associated with the name Kirchhoff-Love ([3] & [4]) in formulations without a separate rotational degree of freedom and with Reissner-Mindlin ([5] & [6]) in formulations with independent rotations (see figure 2).



**Figure 1.** Development of shell concept.

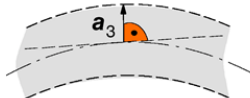
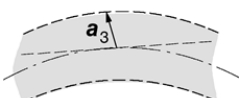
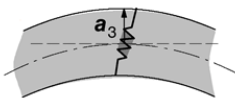
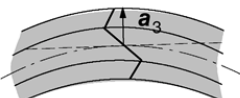
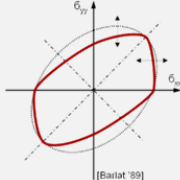
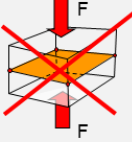
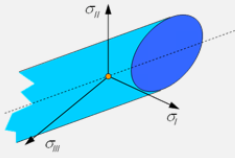
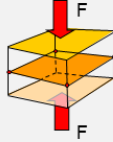
Also three-dimensional shell formulations, including thickness changes are available, but they are practically never used in forming simulations for several reasons. One of them is the lack of feasible constitutive laws. Moreover, the most popular of those, partly available in commercial codes as *solid shells* or *continuum shells*, retain the assumption of transverse fibres remaining straight. For a further, more comprehensive discussion of the topic we refer to the work of Ramm [7], Hauptmann & Schweizerhof [8] and Bischoff et al [9].



**Figure 2.** 3- and 5-parameter shell kinematics.

The overview shown in figure 3 can be used to get a rough classification of shell formulations routinely used in the daily simulation practice, particularly in sheet metal forming. For the geometric description of fibres normal to the shell surface often the vector  $\mathbf{a}_3$  (sometimes denoted as shell director) is introduced. The evolution from so called 3-parameter models to 5-parameter models is outlined for simplicity in the left part of figure 3. The latter describe the deformation of cross-sectional fibres not only by means of three translations but also with the help of two rotational degrees of freedom and thus allow the description of transverse shear deformations. Both models have in

common that loading of the shell surface in normal direction is initially not part of the theory, since a separate degree of freedom to parameterize a strain field in the thickness direction is not provided. Thus, both models cannot provide information about normal stress in thickness direction but *Poisson's* ratio can be used to update at least the thickness of the shell structure. However, with the focus of this contribution being set to limit states like sharp radii and other geometric boundary conditions, like embossing, that introduce normal stresses in thickness direction of the sheet metal, one has to once more emphasize the fact that these stresses are assumed to be zero,  $\sigma_{zz} = 0$ . This eventually yields to reduced constitutive equations that cannot take stresses in thickness direction into account. For the addressed applications, this limitation may lead to severe drawbacks in predictability of part producibility; i.e. the applied shell and constitutive model may not be capable of predicting correct stresses and strains in sharp bends, zero radii or embossing processes.

3-parameter shell model (Kirchhoff-Love)	5-parameter shell model (Reissner-Mindlin)	6- or 7-parameter shell model	Shell model of higher order (multi-layer theories)
			
$ a_3  = \text{const}$	$ a_3  = \text{const}$	$ a_3  = \text{unconstrained}$	
$\sigma_{zz} = 0, (\varepsilon_{zz} = 0)$	$\sigma_{zz} = 0, (\varepsilon_{zz} = 0)$	$\sigma_{zz} \neq 0, \varepsilon_{zz} \neq 0$	$\sigma_{zz} \neq 0, \varepsilon_{zz} \neq 0$
$\gamma_{xz} = \gamma_{yz} = 0$	$\gamma_{xz} \neq 0; \gamma_{yz} \neq 0$	$\gamma_{xz} \neq 0; \gamma_{yz} \neq 0$	$\gamma_{xz} \neq 0; \gamma_{yz} \neq 0$
Straight, unstrained and unwarped fibres; shell director perpendicular w.r.t. shell normal; no shear deformations.	Straight, unstrained and unwarped fibres, shell director rotational w.r.t. shell mid surface, shear deformation possible	Straight and unwarped fibres, straining in thickness direction possible, rotational director.	Shell director may warp, rotate and change length
			
Reduced "2D" stress space	No loading in thickness direction possible	Full 3D stress space	Loading in thickness direction possible

**Figure 3.** Basic classification of shells.

Proposals to enhance the aforementioned shell models, as they have been published for many years in the scientific literature, are available in some commercial software packages, see figure 3 (right). Essentially, additional degrees of freedom to capture deformations and stresses in the thickness direction are introduced. The possibilities for such enhancements are manifold and will not be discussed in detail here. It should be noted, however, that depending on the application, one or the other technology has already proven in practice.

### 3. Limits of classical shell models

A study on the quality of shell elements in sharp bending with small radii in sheet metal forming is provided by Fleischer [10]. Here, a virtual 360° ring, split at the bottom, is pulled displacement controlled apart with constant velocity like a loop or shoelace (compare  $u(t)$  in figure 4, the loading can be considered quasi-static w.r.t. to the investigated phenomena). Constitutive parameters were chosen to represent the steel grade DX54D within a  $J_2$ -plasticity model. One major feature of this virtual test can be seen in the fact that no lateral contact forces need to be transferred onto the shell elements. Two spatial discretizations are being investigated with the finite element package LS-

DYNA® [11] and the element formulations available therein. On the one hand, a plane strain model with 100 continuum elements across the sheet thickness is used. This finely discretized model serves as a reference for further investigations. And on the other hand, several thin shell formulations, i.e. 5p-shell formulations like ELTYP = 1/2/6/7/8/10 or 16 of LS-DYNA®, that are commonly used in engineering practice, are applied. Of course, all these shell discretizations represent the sheet with just one element across the thickness. In thickness direction 9 integration points are used to accurately represent the plastification of the cross section. The characteristic element edge length of the shells is  $l_e=1$  mm. All applied shell elements are based on the same kinematic assumption w.r.t. the loading scenario and deliver – as expected – identical results. The discretization with continuum elements shows that with decreasing residual radius in the loop vertex (see figure 5), the isochoric (volume preserving) characteristic of the underlying  $J_2$ -based constitutive model leads to a substantial cross-sectional warping. This is accompanied by a shift of the neutral axis where  $\sigma_{xx}=0$  or equivalently of the stress maximum  $\sigma_{zz}$  (see figure 5, right) towards the inner surface marked by the blue dot.

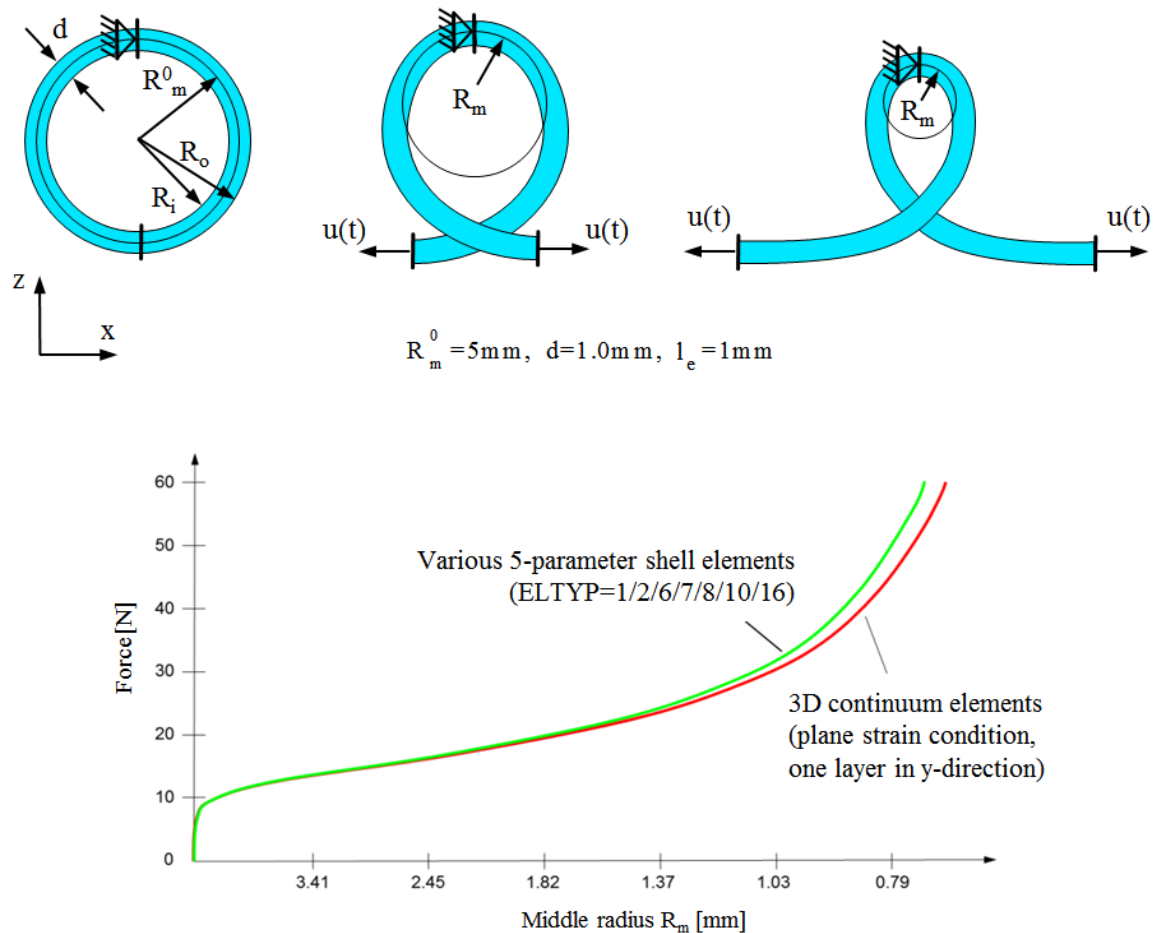


**Figure 4.** Geometry and force vs. radius result of the virtual ring test.

As already stated above: Both effects cannot be reproduced by the applied shell elements, since on the one hand by assuming unwarped fibres, the corresponding deformations are no longer correctly represented and on the other hand significant stresses in thickness direction are not part of the solution space of such shell elements. As a consequence, the global force-displacement relationship shows a significant deviation from the continuum solution below a loop radius of approximately 1 mm. While such deviation may be tolerable for a global assessment of manufacturability, the corresponding local deformation may be restricted severely leading to intolerable, local inaccuracies. In case one focuses

on damage and failure prediction, which typically builds on correct representation of stresses and strains in the applied spatial discretization, such deviations are prohibitive.

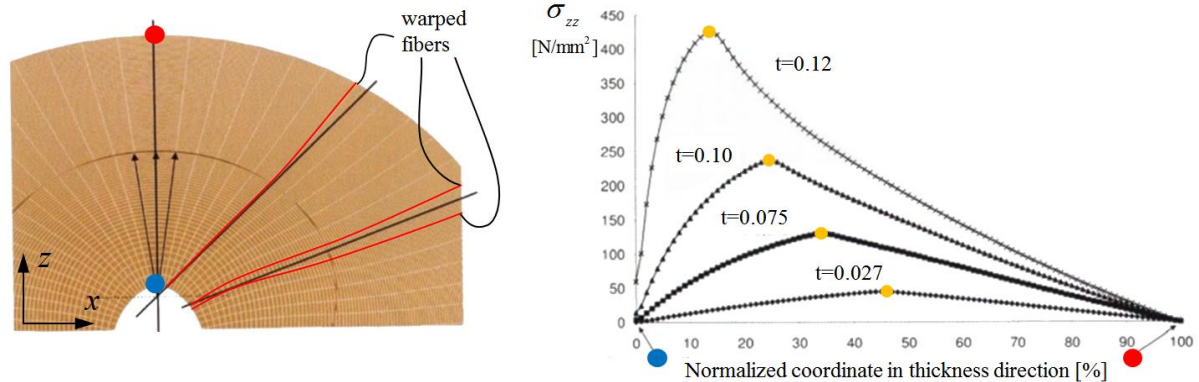


**Figure 5.** Deformation of fibres in thickness direction (left). Stress distribution in thickness direction at different loading stages (right).

#### 4. Plate bending test

Very similar to the virtual ring geometry present in the previous section, the plate bending test according to VDA 238-100 is now carried out. Here, a punch that introduces lateral contact forces onto the shell discretized structure needs to be taken into account. As can be seen in figure 6 a fine spatial discretization with 16 volume elements across the thickness serves as reference solution. Trilinear hexahedron elements (ELTYP=2 of LS-DYNA<sup>®</sup>) with an edge length of  $l_e=0.125$  mm leading to a sheet thickness of 2.0 mm are used. Explicit time integration is applied. However, the nature of the time integration scheme is irrelevant for the present study. In the following the stress state characteristics that are computed by different element formulations are compared. The investigation is motivated by the fact that a number of commercially used damage and failure concepts like the generalized Johnson-Cook or GISSMO model (Johnson & Cook [12], Andrade et al. [13]) or the bi-failure concept (Andrieux [14]) are based on the stress invariant measures *triaxiality*  $\eta$  and *Lode angle*  $\xi$ .

$$\eta = -\sigma_{ii} / (3\sigma_{vm}) \text{ and } \xi = -\frac{27}{2} \frac{J_3}{\sigma_{vm}^3} \quad (1)$$

Here  $\sigma_{vm}$  represents the von Mises stress and  $J_3$  the third invariant of the stress deviator. It needs to be noted that other damage and fracture models that for instance are based on in-plane strain invariants (Liewald & Drotleff [15] or Volk & Suh [16]) may be less sensitive but may in the limit state still suffer from inaccurate strain representation in the necking region as well.

It is well known that classical 5-parameter shell models are able to provide values of  $\eta$  and  $\xi$  that correspond to a plane stress state (and are therefore not independent of each other) while shell formulations that are enhanced with whatever degree of freedom in thickness direction are, in principle, able to better and more accurately represent the three-dimensional stress and strain conditions in the shell space. In the following, a *von Mises* or  $J_2$ -plasticity constitutive model is used which is available for 5-parameter shell elements as well as for 3D discretizations, either continuum or enhanced shell formulations. The yield curve has been chosen to represent a DP600 steel grade. It should be emphasized, however, that the result of the present study is independent of the constitutive model; we only set focus on the fact that yielding actually takes place during loading and *Poisson's* ratio  $\nu$  thus changes from an initial value of 0.3 to 0.5 due to plastic loading. In all virtual tests, the punch was displacement controlled up to a travel of 13 mm. Figure 6 (left) shows the basic structure of the virtual experiment discretized with continuum elements, the corresponding fringe plot, the plastic

strains at the end of punch travel and the evaluation of the stress invariant measures *triaxiality*  $\eta$  and *Lode angle*  $\zeta$  therein.

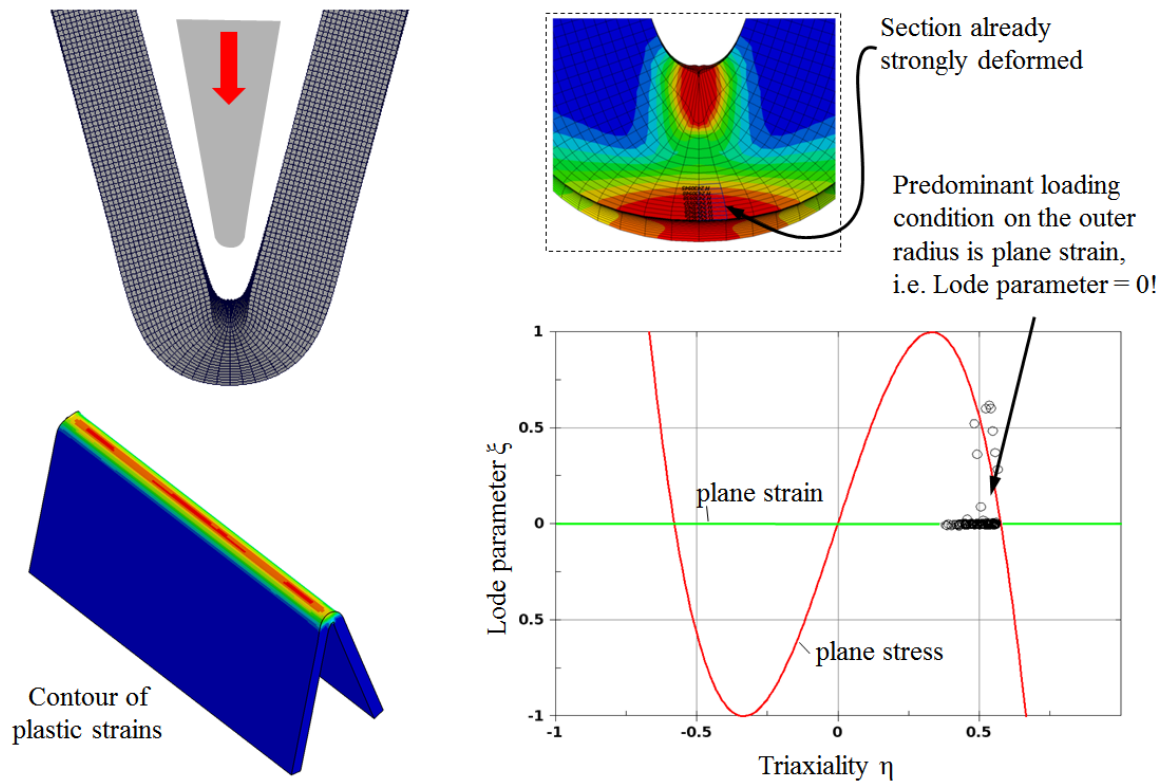


**Figure 6.** Volume discretization of plate bending test.

In the *Lode parameter* vs. *triaxiality* diagram ( $\zeta$ - $\eta$  diagram, see figure 6, right), where the marks depict dimensionless data to characterize the stress states on the outer surface at the end of punch travel, it can be clearly seen that a plane strain state predominates in the outer, near-surface region. In addition, a cross-section warping is observed as discussed in the virtual ring experiment of the previous section. In the following, common shell formulations are compared with this continuum discretization. First, a fully integrated, bi-linear shell element (ELTYP=16, IDOF=1 of LS-DYNA®) with a characteristic edge length of  $l_e=0.125$  mm is applied. Figure 7 shows the basic structure and the generated stress invariant measures of randomly selected points along the bead in  $\zeta$ - $\eta$  space again at the end of punch travel of the virtual experiment. Evaluated and depicted by rectangular and triangular marks are stress states across the thickness in the bend only. As expected, the 5-parameter shell element delivers stress invariant measures that correspond to a plane stress state only. Thus, the actual state of stress in the bending radius is predicted inaccurately for very small radii. In particular, the lateral compressive stresses acting via the punch, as documented in figure 6, are not taken into account by this shell formulation.

An ad-hoc engineering solution to the problem can be found in recent releases of commercial finite element codes. Here, the effect of the lateral acting punch on the stress state in the shell element is approximated by superimposing the contact forces across the shell thickness onto the respective integration points (ELTYP=16, IDOF=3 in LS-DYNA®). The following ansatz for  $\sigma_{zz}$  is being made:

$$\sigma_{zz} = \alpha \left( \frac{\sigma_c^b - \sigma_c^t}{4} (z^3 - 3z) - \frac{\sigma_c^b - \sigma_c^t}{2} \right), \quad (2)$$

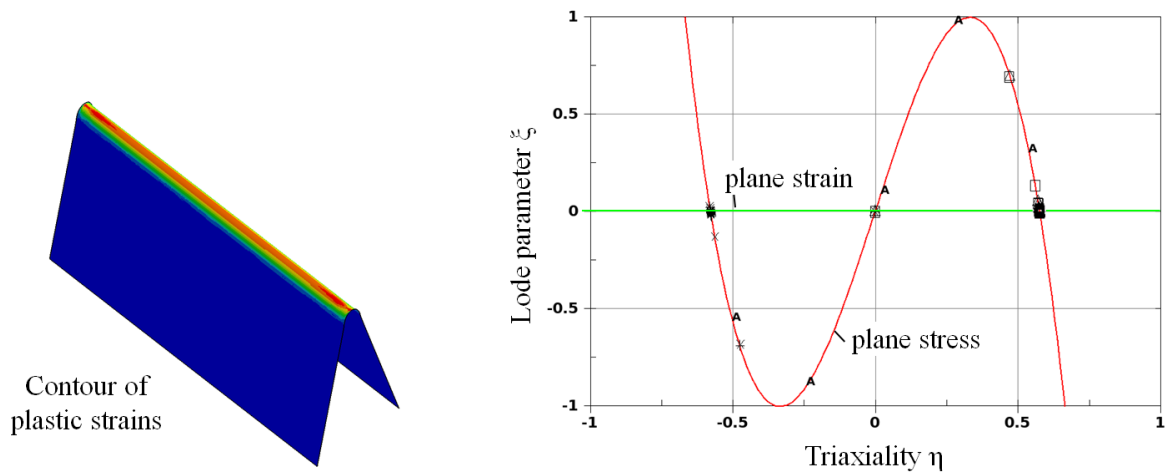


**Figure 7.** Virtual plate bending test with 5-parameter shells. Different marks represent values of  $\xi$ - $\eta$  at end of punch travel in the bend section across the thickness.

where  $\sigma_c^t$  and  $\sigma_c^b$  are the respective surface stresses collected from the contact algorithm at the top and the bottom of the shell element respectively.  $\alpha$  is a numerical parameter and  $z$  is the local variable in shell space in thickness direction. The lateral acting contact stresses occurring at the shell outer surfaces are distributed to the integration points with the help of (2) and iteratively added to the internally acting stresses. The result of this stress overlay is depicted in figure 8. It can be seen that now also stress states outside the plane stress condition occur and the stress invariant measures in tension also take values close to  $\xi=0$ , which denotes plane strain conditions. Hence the state of stress in the shell section may represent the real conditions better. However, it must be noted that an external stress component due to surface contact is necessary in this case. Lacking this condition, for example if the deformation is applied due to pure local bending, this engineering approach fails. The results would then correspond to those of a 5-parameter formulation without any such modification.

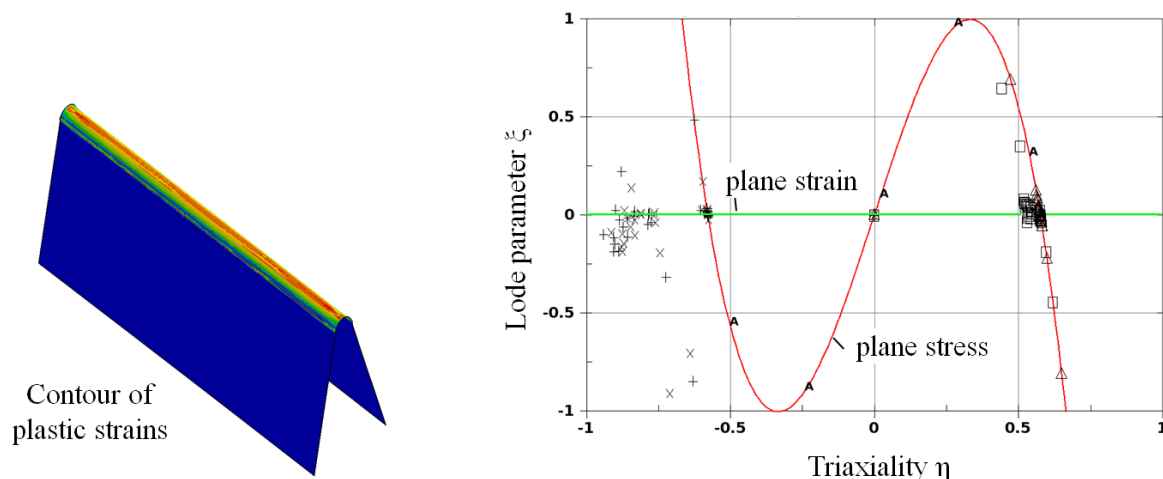


**Figure 8.** Virtual plate bending test with 5-parameter and stress modification due to lateral contact. Different marks represent values of  $\xi$ - $\eta$  at end of punch travel in the bend section across the thickness.

In a next step, it will be investigated to what extent so-called layered *thick* shell formulations in a commercial finite element code (ELTYP=5 in LS-DYNA®) can solve the aforementioned problem. Such layered discretizations allow a piecewise linear warping of the cross section in the thickness direction in the same sense as the continuum discretized reference solution provided earlier in the

present section. In this case, 5 thick shell elements were stacked in thickness direction. It can thus be expected that the cross-sectional warping and the displacement of the zero stress axis of the cross section below the punch can be well captured by this approach.

Comparing the corresponding analysis results in figure 9, it can be seen that the results are already in good agreement with the converged continuum solution. However, it should not go unmentioned that the number of degrees of freedom has increased significantly compared to the classical single-layer 5-parameter shell discretization. It must also be noted that the critical time step in simulations with an explicit time stepping schemes depends on the characteristic element length. The latter is dominated in the case of *thick* shell formulations by the thickness direction and is therefore significantly smaller compared to classical shell elements.

Yet another possible solution to the general issue can be found in the literature as so-called 7-parameter shell formulations (see, for example, Büchter et al. [17], Cardoso & Yoon [18]) or solid shell formulations (e.g. Hauptmann & Schweizerhof [8]). These formulations introduce two additional degrees of freedom in thickness direction and therefore allow the representation of a linear transverse normal strain field and the corresponding independent displacement of the neutral surface. One possibility to introduce a linearly varying thickness strain is the following quadratic approach for  $u_z$  in the thickness direction:

$$u_{z,i} = \frac{z}{2} t_i - (1 - z^2) q_i \quad (3)$$

Here,  $z$  represents the local coordinate in thickness direction of the element,  $t$  and  $q$  stand for the two additional degrees of freedom for the corresponding node  $i$ . For the sake of completeness, it should be mentioned that in the absence of a quadratic term in favour of a linear displacement the corresponding strain field in the  $z$  direction will not allow a shift of the neutral axis from the geometrical centre. This constraint leads to strong *Poisson*-thickness locking. Hence corresponding formulations are not recommended at all.

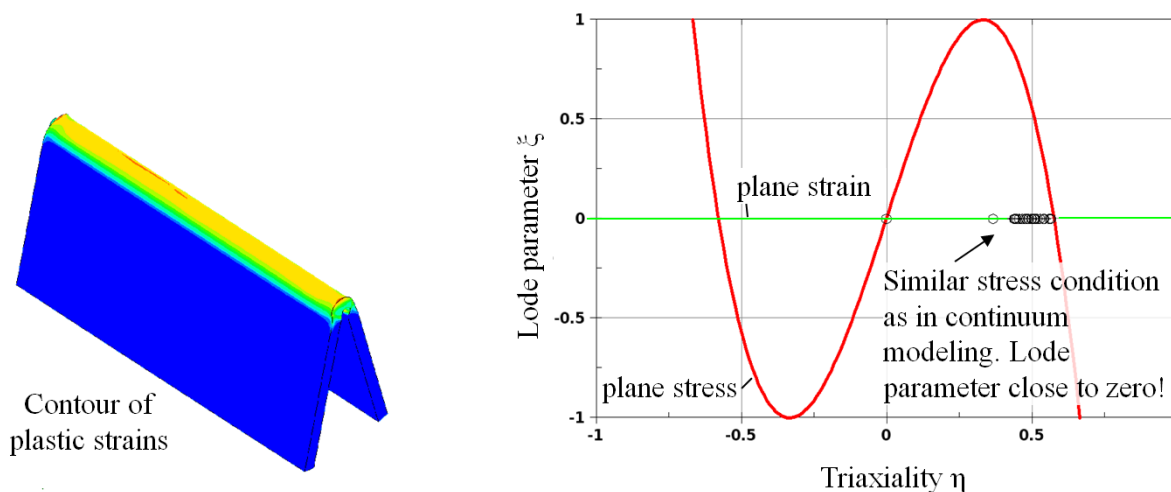


**Figure 9.** Virtual plate bending test discretized with 5 thick shell elements across the thickness direction. Marks represent values of  $\xi$ - $\eta$  at end of punch travel on the outer surface in the bend section.

However, it can be seen in the following that the 7-parameter formulation as currently available in LS-DYNA® (ELTYP=25/26) also reach an application limit if large cross-sectional deformations in combination with changing *Poisson*'s ratio are required. For the plate bending test considered here, the assumption of straight, undeformed fibres and, in particular, the linear approximation of the strains in thickness direction provide an inner constraint, which subsequently leads to insufficient stress prediction.

The latter is even more pronounced in the present example, since the isochoric behaviour triggered by the constitutive model, once plastic loading takes place, would require a higher order strain approximation in thickness direction. Clearly, this cannot be captured by the linear strain ansatz. Figure 10 shows this problem again in the  $\xi$ - $\eta$  diagram. Although one would actually expect that the 3D-7-parameter shell model should lead to an improved solution for the stress state, the points of the stress invariant measures are widely scattered. The insufficient approximation of the strain field in thickness direction ultimately provides incorrect stress results.

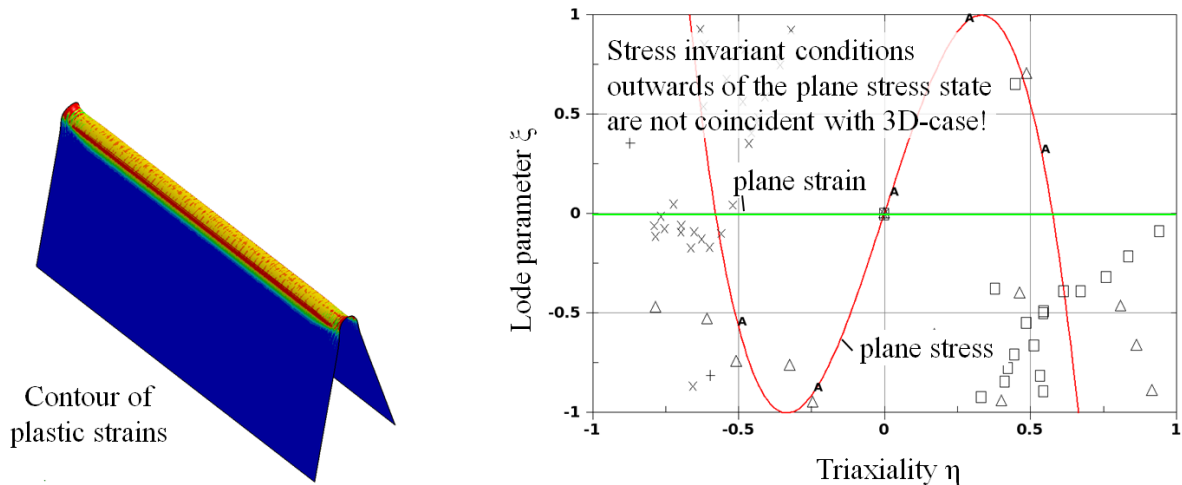


**Figure 10.** Virtual plate bending test with 7-parameter shell elements and scattered data.

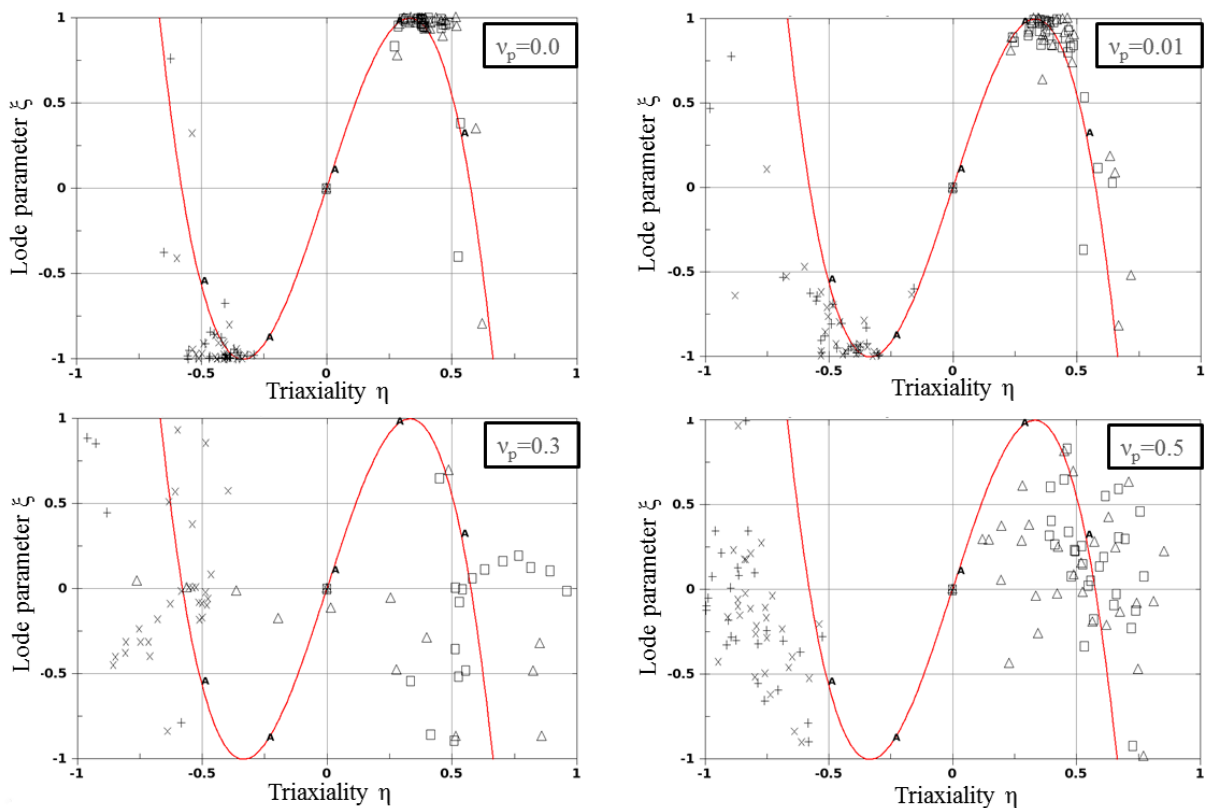


**Figure 11.** Virtual plate bending test discretized with 7-parameter shell elements and varying Poisson's ratio. Again, different marks represent values of  $\xi$ - $\eta$  at end of punch travel in the bend section across the thickness.

It should be noted, however, that the error is very much due to the isochoric constitutive behaviour or more precisely due to the transition of the *Poisson's* ratio from elastic ( $\nu=0.3$ ) to plastic behaviour ( $\nu_p=0.5$ ) and the therefore required higher nonlinearity in normal strains distribution. The latter conclusion can be proven numerically by applying a constitutive model that allows a variable definition of *Poisson's* ratio number once plastic loading takes place. Here for example MAT\_187 / SAMP in LS-DYNA® may be applied. In figure 11 the results of a model with differently chosen but constant *Poisson's* ratio  $\nu_p$  in the plastic loading regime are shown. Clearly, the specification of  $\nu_p$  with unmodified yield locus and unmodified yield curve redefines the direction of the plastic flow, i.e. the plastic potential. The plastic *Poisson's* ratio was varied from  $\nu_p=0.0$  to  $\nu_p=0.5$  in 4 steps. It can be observed that with increasing  $\nu_p$  the unphysical deviation in the invariant stress measures increase. At  $\nu_p=0.0$  there is a plausible picture of the stress invariants but it must be noted that the material behaviour in this case ultimately corresponds to that of a foam.

## 5. Summary

In this paper, shell models available in virtually every general purpose finite element code have been critically discussed in view of the demanding applications in sheet metal forming. Especially with very small radii, as in beads, edges and embossing applications, the assumptions of straight fibres and zero normal stress hypothesis in thickness direction of classic 5-parameter shell formulations reach their limit. Great losses in accuracy may be the result, especially when damage and fracture are regarded. As a remedy, the use of 7-parameter formulations may help to a limited extent, since these formulations typically have a linear transverse normal strain approximation in thickness direction. The latter may be sufficient for elastic structures at moderate strains, but for locally concentrated plastic deformations this provides a constraint that leads to questionable results, irrespective of the software code used. The only solution remains to discretize the corresponding structures with a sufficient number of layered *thick* shell elements. The overhead in computation time has to be accepted.

Ultimately, the question for a meaningful (further) development of shell elements arises. In the opinion of the authors, shell formulations with higher order strain approximations in thickness direction are one way to counteract the indicated loss of accuracy. However, further research is needed to reconcile accuracy, modelling and numerical complexity, as well as efficiency.

It must also be emphasized at this point that the use of *thick* shells introduces as well full three-dimensional stress-strain relationships which in turn implies that many highly developed constitutive relationships used at present need fundamental reconsideration. Many constitutive models used in sheet metal forming simulation are based on the assumptions of a plane stress state. Consequently, correspondingly reduced experimental investigations suffice for calibration. However, with the availability of (and the necessity to use) full three-dimensional stress-strain relationships, not only new constitutive models but also new calibration procedures are in high demand.

## Acknowledgements

The present study was supported within project No. 09/117 of the European Research Association for Sheet Metal Processing e.V. and as project No. 19797N within the framework of the AiF (Program for the Promotion of Industrial Community Research of the Federal Ministry for Economic Affairs and Energy) of Germany.

## References

- [1] Ahmad S, Irons B M and Zienkiewicz OC, Analysis of thick and thin shell structures by curved finite elements, *International Journal for Numerical Methods in Engineering* 2 (1970), 419-451.
- [2] Koiter W T, Consistent, first approximation in the general theory of thin elastic shells, in Koiter W T et al. (1960), *The theory of thin elastic shells*, North-Holland, Amsterdam, 12-33.

- [3] Kirchhoff G, Über das Gleichgewicht und die Bewegung einer elastischen Scheibe, *Journal für die reine angewandte Mathematik*, 40 (1850), 51-58.
- [4] Love A E H, On the small vibrations and deformations of thin elastic shells, *Philosophical Transactions of the royal Society*, 179 (1888), 491 ff.
- [5] Reissner E, The effect of transverse shear deformation on the bending of elastic plates, *Journal of Applied Mechanics*, 12 (1945), 69-76.
- [6] Mindlin R D, Influence of rotary inertia and shear on flexural motions of isotropic elastic plates, *Journal of Applied Mechanics* 18 (1951), 31-38.
- [7] Ramm E, A plate/shell element for large deflections and rotations, in *Formulations and Computational Algorithms in Finite Element Analysis* (eds. K.J. Bathe et al.), M.I.T. Press, 1977.
- [8] Hauptmann R and Schweizerhof K, A systematic development of solid-shell element formulations for linear and non-linear analyses employing only displacement degrees of freedom, *Int. J. Num. Meth. Eng.* 42 (1998), 49-69.
- [9] Bischoff M, Ramm E and Irlinger J, 2017, Models and Finite Elements for Thin-Walled Structures. in *Encyclopedia of Computational Mechanics Second Edition*, eds. Stein E, de Borst R and Hughes T J, doi:10.1002/9781119176817.ecm2026
- [10] Fleische, M, Absicherung der virtuellen Prozesskette für Folgeoperationen in der Umformtechnik, Band 12, Schriftenreihe des Lehrstuhls für Statik, TU München, ISBN 978-3-8322-8398-8, deutsch.
- [11] LS-DYNA® Keyword Users's Manual, Version R8.1, Livermore Software Technology, Corporation (LSTC), 2016.
- [12] Johnson G R and Cook W H, Fracture characteristics of three metals subjected to various strains, strain rates, temperatures and pressures, *Engineering Fracture Mechanics*, Vol. 21(1), 1985, S. 31-48.
- [13] Andrade F X C, Feucht M, Haufe and Neukamm F, An incremental stress state dependent damage model for ductile failure prediction, *Int. J. Fract.*, DOI 10.1007/s10704-016-0081-2.
- [14] Andrieux F, Von Mises model with bi-failure criterion, User subroutine for LS-DYNA® 971R3, Fraunhofer IWM, internal report, 2008.
- [15] Liewald M and Drotleff K, Bewerten von Umformgrenzen bei nicht-linearen Beanspruchungen in der Praxis, EFB-Forschungsbericht Nr. 428, Institut für Umformtechnik der Universität Stuttgart, ISBN 978-3-86776-475-9.
- [16] Volk W and Suh J, Prediction of formability for non-linear deformation history using generalized forming limit concept (GFLC), NUMISHEET 2014 2013, 2013.
- [17] Büchter N, Ramm E and Roehl D, Three-dimensional extension of nonlinear shell formulation based on the enhanced assumed strain concept, *Int. J. Numer. Meth. Eng.*, 37:2551–2568, 1994.
- [18] Cardoso R P R and Yoon J W, One point quadrature shell element with through-thickness stretch, *Computer Methods in Applied Mechanics and Engineering*, 194, 1161.